

The Effect of Surgical Technique and Spacer Texture on Bone Regeneration: A Caprine Study Using the Masquelet Technique

Viviane Luangphakdy MS, G. Elizabeth Pluhar DVM, PhD, Nicolás S. Piuizzi MD, Jean-Claude D'Alleyrand MD, Cathy S. Carlson DVM, PhD, Joan E. Bechtold PhD, Jonathan Forsberg MD, PhD, George F. Muschler MD

Received: 30 November 2016 / Accepted: 12 June 2017 / Published online: 20 June 2017
© The Association of Bone and Joint Surgeons® 2017

Abstract

Background The Masquelet-induced-membrane technique is a commonly used method for treating segmental bone defects. However, there are no established clinical standards for management of the induced membrane before grafting.

Questions/purposes Two clinically based theories were tested in a chronic caprine tibial defect model: (1) a textured spacer that increases the induced-membrane surface area will increase bone regeneration; and (2) surgical scraping to remove a thin tissue layer of the inner induced-membrane surface will enhance bone formation.

Methods Thirty-two skeletally mature female goats were assigned to four groups: smooth spacer with or without membrane scraping and textured spacer with or without membrane scraping. During an initial surgical procedure (unilateral, left tibia), a defect was created excising bone (5 cm), periosteum (9 cm), and muscle (10 g). Segments initially were stabilized with an intramedullary rod and an antibiotic-impregnated polymethylmethacrylate spacer with a smooth or textured surface. Four weeks later, the spacer was removed and the induced-membrane was either scraped or left intact before bone grafting. Bone formation was assessed using micro-CT (total bone volume in 2.5-cm

This work was funded by the Congressionally Directed Medical Research Programs Peer Reviewed Orthopaedic Research Program grant Award # W81XWH-13-2-0086 (GFM).

All ICMJE Conflict of Interest Forms for authors and *Clinical Orthopaedics and Related Research*® editors and board members are on file with the publication and can be viewed on request. *Clinical Orthopaedics and Related Research*® neither advocates nor endorses the use of any treatment, drug, or device. Readers are encouraged to always seek additional information, including FDA-approval status, of any drug or device prior to clinical use. Each author certifies that his or her institution approved the animal protocol for this investigation and that all investigations were conducted in conformity with ethical principles of research. Some of the authors (JCA and JF) are employees of the US Government. This work was prepared as part of their official duties. Title 17 U.S.C. §105 provides that “Copyright protection under this title is not available for any work of the United States Government.” Title 17 U.S.C. §101 defined a US Government work as a work prepared by a military service member or employees of the US Government as part of that person’s official duties. The opinions or assertions contained in this paper are the private views of the authors and are not to be construed as reflecting the views, policy or positions of the Department of the Navy, Department of Defense, nor the US Government.

This work was performed at Cleveland Clinic, Cleveland, OH, USA.

Electronic supplementary material The online version of this article (doi:10.1007/s11999-017-5420-8) contains supplementary material, which is available to authorized users.

N. S. Piuizzi, G. F. Muschler (✉)

Department of Orthopaedic Surgery and Biomedical Engineering (ND20), Lerner Research Institute, Cleveland Clinic, 9500 Euclid Avenue, Cleveland, OH 44195, USA
e-mail: muschlg@ccf.org

V. Luangphakdy

Department of Biomedical Engineering, Lerner Research Institute, Cleveland Clinic, Cleveland, OH, USA

G. Elizabeth Pluhar

Department of Veterinary Clinical Sciences, College of Veterinary Medicine, University of Minnesota, Saint Paul, MN, USA

N. S. Piuizzi

Instituto Universitario del Hospital Italiano de Buenos Aires, Buenos Aires, Argentina

central defect region) as the primary outcome; radiographs and histologic analysis as secondary outcomes, with the reviewer blinded to the treatment groups of the samples being assessed 12 weeks after grafting. All statistical tests were performed using a linear mixed effects model approach.

Results Micro-CT analysis showed greater bone formation in defects with scraped induced membrane (mean, 3034.5 mm³; median, 1928.0 mm³; quartile [Q]1–Q3, 273.3–2921.1 mm³) compared with defects with intact induced membrane (mean, 1709.5 mm³; median, 473.8 mm³; Q1–Q3, 132.2–1272.3 mm³; $p = 0.034$). There was no difference in bone formation between textured spacers (mean, 2405.5 mm³; median, 772.7 mm³; Q1–Q3, 195.9–2743.8 mm³) and smooth spacers (mean, 2473.2 mm³; median, 1143.6 mm³; Q1–Q3, 230.2–451.1 mm³; $p = 0.917$).

Conclusions Scraping the induced-membrane surface to remove the innermost layer of the induced-membrane increased bone regeneration. A textured spacer that increased the induced-membrane surface area had no effect on bone regeneration.

Clinical Relevance Scraping the induced membrane during the second stage of the Masquelet technique may be a rapid and simple means of improving healing of segmental bone defects, which needs to be confirmed clinically.

Introduction

Segmental bone defects represent a major, unsolved clinical challenge in orthopaedic practice, in civil and military populations [3, 4, 18, 21, 23]. Bone defects may result from high-energy trauma, infection, tumor resection, or revision surgery [3, 6, 11, 17, 25]. Although acute bone shortening may be performed for the treatment of small defects between 1 and 3 cm, autogenous cancellous bone graft

remains the gold standard treatment for bone defects less than 5 cm [17, 23]. For larger bone defects, early grafting with autogenous cancellous bone graft results in a risk of nonunion resulting from graft resorption and lack of consolidation [11, 17, 23]. Therefore, alternative approaches have been described, including distraction osteogenesis, vascularized bone transfer, the induced-membrane technique (commonly called the Masquelet technique), and amputation [2, 3, 11, 17, 23].

Masquelet et al. [14, 15] developed a technique to repair large bone defects in two surgical steps. In the first step, débridement and placement of a polymethylmethacrylate (PMMA) cement spacer loaded with antibiotics with soft tissue coverage if required is done. This first procedure is stabilized using an intramedullary rod or plate fixation. In the second step, performed 4 to 8 weeks later, the PMMA spacer is removed and bone graft material is placed in the soft tissue envelope that has formed around the spacer (ie, the induced membrane) [13–16]. Although this technique has a high clinical success rate, it usually demands multiple additional interventions to obtain bone union, and has a 10% to 15% failure rate [2, 13, 21]. In 2016, Masquelet stated that the best combination between an induced membrane and the osteoinductive and osteoconductive material put inside the membrane remained undetermined [13].

Large-animal models offer an important platform in targeting the improvement of strategies for bone regeneration. Standardized and well-characterized, reproducible, and clinically relevant models are essential to generate preclinical data required to advance therapeutic strategies in clinical practice.

The chronic caprine tibial defect model is a segmental bone defect animal model that better represents the complexity and severity of the actual biologic environment in which clinical bone grafts currently fail. Using the chronic caprine tibial defect model, we tested two modifications of the Masquelet induced-membrane technique to evaluate if they enhanced bone formation by: (1) scraping the inner layer of the induced membrane to remove tissue involved in the foreign body reaction and to induce bleeding in the vascular tissue bed; and, (2) the use of a textured spacer to increase the surface area for diffusion and revascularization arising from the induced membrane. These technical surgical modifications may represent a rapid and simple means of enhancing the biologic environment of the induced-membrane tissue bed. Therefore this study presents two theories: (1) the use of a textured spacer that doubles the inner surface area of the induced membrane during the first stage of the Masquelet induced-membrane technique, will increase bone formation after grafting; and (2) surgical scraping to remove a thin (1–2 mm) layer of the inner surface of the induced membrane immediately

J.-C. D'Alleyrand
Department of Surgery, Orthopaedics, Walter Reed National
Military Medical Center, Bethesda, MD, USA

C. S. Carlson
Department of Veterinary Population Medicine, College of
Veterinary Medicine, University of Minnesota, Saint Paul, MN,
USA

J. E. Bechtold
Department of Orthopaedic Surgery, Minneapolis Medical
Research Foundation and University of Minnesota, Saint Paul,
MN, USA

J. Forsberg
Regenerative Medicine Department, Naval Medical Research
Center, Silver Spring, MD, USA

adjacent to the spacer will enhance bone formation after bone grafting.

Materials and Methods

Thirty-two skeletally mature female goats, 5 ± 1 years old (mean \pm SD), weighing 50 ± 4 kg underwent the chronic caprine tibial defect procedure and were randomly assigned to four groups (eight animals/group) using a two-by-two test matrix (factorial design). These groups included (1) smooth spacer and intact induced membrane; (2) smooth spacer and scraped induced membrane; (3) textured spacer and intact induced membrane; and (4) textured spacer and scraped induced membrane. Study animals were cared for in accordance with the principles of the *Guide for the Care and Use of Laboratory Animals* [20] after approval from the Cleveland Clinic Institutional Animal Care and Use Committee (IACUC #2013-1021) and the Animal Care and Use Review Office of US Army Medical Research and Materiel Command (OR #120082).

Three goats were excluded owing to complications. Two belonged to the intact and smooth group and were excluded owing to *Staphylococcus epidermidis* infection ($n = 1$) or caseous lymphadenitis ($n = 1$); one goat in the scraped and smooth group was excluded because of an anesthetic complication during Stage 2 surgery ($n = 1$).

Chronic Caprine Tibial Defect Model

Before each surgery, goats were given perioperative analgesia using staged application of transdermal fentanyl patches (each $50 \mu\text{g}/\text{hour}$). Medetomidine ($0.025 \text{ mg}/\text{kg}$ intramuscular) and ketamine ($0.5\text{--}1.0 \text{ mg}/\text{kg}$ intramuscular) were given for anesthetic induction to place an endotracheal tube and anesthesia was maintained with isoflurane 1.0% to 2.0% in oxygen. Cefazolin, 1 g intravenous, was given prophylactically just before and at the end of surgery. Morphine ($0.1 \text{ mg}/\text{kg}$), diluted in 0.9% sterile saline to a volume of $0.13 \text{ mL}/\text{kg}$, was given for analgesia in the epidural space after induction.

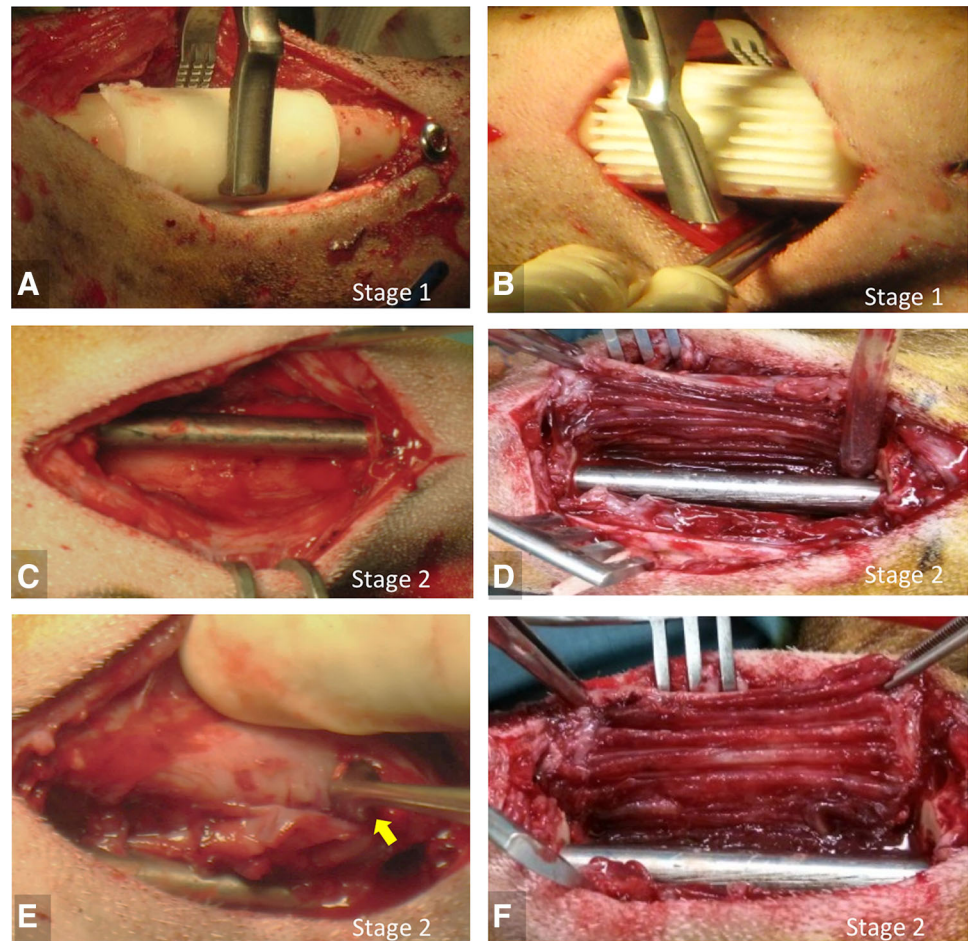
The first surgical procedure consisted of two procedures: (1) creation of the critical bone defect in the left tibia; and (2) “spacer procedure” or “Stage 1” of the Masquelet technique. During the first procedure, a medial approach was made to the left tibia. A 5-cm mid-diaphyseal osteoperiosteal segment was removed beginning 6.5 cm above the medial malleolus. Additional 2-cm segments of periosteum were removed on both sides of the defect and 10 g (approximately 10 cm^3) of skeletal muscle surrounding the defect site. Gelpi retractors were used proximally and distally to uniformly expose the muscle

surfaces around the defect gap. Electrocautery was used to remove sheets of muscle 2 to 5 mm thick around all surfaces of the defect. When encountered, tendon tissue was preserved to limit the risk of muscle segment discontinuity. In general, 6 to 7.5 g of the cranial tibialis muscle and 2.5 to 4 g of gastrocnemius muscle were removed. Excised tissue was placed in a tarred dish on a digital scale until a total of 10 g of tissue had been removed. Following this débridement, the muscle surface around the defect was essentially devoid of normal muscle surfaces. The tibia was stabilized with an 8-mm diameter, 185-mm long intramedullary interlocking nail (Innovative Animal Products, Rochester, MN, USA) and the defect was filled with a PMMA cement spacer impregnated with vancomycin (0.5 g) and tobramycin (0.5 g) (Simplex™ P polymer; Stryker, Mahwah, NJ, USA) (diameter 2.1 cm). As indicated previously, 16 goats were assigned to the smooth spacer group (Fig. 1A) and the remaining 16 goats were assigned to the textured spacer group (Fig. 1B) during this first procedure. The textured spacer was fabricated with 2-mm thick and 2-mm deep linear grooves, which doubled the effective surface area of the spacer and the resulting induced membrane.

The second surgical procedure (“grafting procedure” or “Stage 2” of the Masquelet technique) was performed 4 weeks later. The PMMA spacer was removed through a medial approach using a “bomb bay door” (ie, “H” shaped incision) opening technique (Fig. 1C, D). In the intact induced-membrane group, the inner induced-membrane layer was left intact ($n = 16$ goats) (Fig. 1C, D). In the scraped induced-membrane group, the inner layer of the induced membrane was removed with a curette ($n = 16$ goats) comprising the loosely adherent zone of foreign body reaction around the spacer, exposing a more-fibrous surface of dense connective tissue in the induced membrane (Fig. 1E, F). Subsequently the defect in all cases was filled with 10 to 12 cm^3 of autogenous cancellous bone graft harvested from the sternum. The sternum was exposed using a lateral parasternal approach through normal skin, avoiding the thick and callused skin and dense avascular fat pad over the midline of the sternum on which the goat rests when recumbent. A subperiosteal approach is used, passing under and elevating the fat pad. The ventral aspect of the sternum was decorticated, and gouges and curettes were used to harvest autogenous cancellous bone graft in pieces measuring 2 to 4 mm in diameter, preserving the fibrous intersternbral segments and the dorsal cortex. The induced membrane and skin were separately closed with $3\text{--}0$ polydioxanone and nylon, respectively.

Postoperative pain management was administered using transdermal fentanyl patches ($100 \mu\text{g}/\text{hour} \times 5$ days) and phenylbutazone (1 g orally). Animals were allowed to be freely mobile and fully weightbearing immediately on

Fig. 1A–F The intraoperative photographs show placement of a (A) smooth spacer and (B) textured spacer in the defect site during the “spacer procedure” (Stage 1, Masquelet technique). Four weeks later during the “grafting procedure” (Stage 2, Masquelet technique), the induced membrane is appreciated after removal of the (C) smooth and (D) textured spacers. Scraping the inner layer of the induced membrane with a curette (yellow arrow) was done in half of the goats from the (E) smooth and (F) textured spacer groups.



recovery from anesthesia. They were housed in individual pens with free access to food and water. The goats were checked twice daily for mentation and attitude, ability to ambulate, willingness to bear weight on the surgically treated limb, food and water consumption, respiratory rate, and inflammation at the surgical site.

The goats were euthanized 12 weeks after the second surgical procedure (Stage 2 of the Masquelet technique), and the entire left tibia was harvested, preserving the periosteum and fibrous tissue surrounding the defects. Samples were fixed in 10% neutral buffered formalin for 48 hours and then transferred to 70% ethanol where they were kept until micro-CT was done, followed by histologic analysis.

Micro-CT Processing and Analysis

High-resolution micro-CT was used for the primary outcome measures of amount and distribution of bone in each defect. Before scanning, the nail and screws were carefully removed and replaced with a radiolucent rod and cross-pins

to maintain the original length and axial and rotational alignment. After centering in the scanner (Inveon® microCT scanner; Siemens Medical Solutions, Knoxville, TN, USA), 441 projection images were acquired at 0.5°-increments at 39- μm isotropic voxel size (80 kVp; 500 μA). Data were reconstructed in three-dimensional (3-D) volumes using a modified tent-Feldkamp-Davis-Kress algorithm [9], and calibrated to mg/cm^3 of hydroxyapatite using an air, water, and hydroxyapatite phantom scanned under the same conditions. Bone threshold was set at 1300 mg hydroxyapatite/ cm^3 (747 Hounsfield units [HU]). The analyzed volume of interest included the 5-cm defect region plus 1 cm of bone proximal and distal to the defect. Each specimen was analyzed with segmentation software developed in-house, in which a 3-D cylindrical “defect template” volume, 45 mm in diameter and 70 mm in length, was manually positioned to define the boundaries of the volume of interest. The reviewer (TZ) was blinded to the treatment groups of the samples being assessed. Primary outcome was defined as total bone volume (tBV) in the central 2.5-cm region of the defect, which is the most challenging region to heal. Secondary outcomes were

radial percent bone volume (%BV), a summation of circumferential bone volume over the length of the 5-cm defect, and moment angle of inertia. The moment angle of inertia is calculated for each slice through the defect as the sum of the product of mineral density distance from the centroid for each pixel in the slice. Summary data of the pattern and extent of mineralization in the defects in each group were illustrated by projecting %BV versus radial position using a two-dimensional (2-D) color map ranging from 0% (purple) to 60% (red). The x-axis indicated distance from the center of the medullary canal to the periosteal surface (range, 0–29 mm). The y-axis represented the position in the long axis of the bone (range, 0–70 mm) including the 5-cm defect plus 1 cm proximal and distal. Mean moment angle of inertia for each group also was plotted using a 2-D color plot color map ranging from 0 (dark blue) to 7000 (red) in $\text{HU} \cdot \text{mm}^2$ plotted about the bone circumference in the x-axis and the long bone axis position in the y-axis. The moment angle of inertia plot is used to illustrate the radial distribution of new bone (x-axis indicates radial distribution with respect to anatomic radial quadrants, ie, anterior, medial, lateral, posterior, lateral) at any vertical position in the defect.

Radiographic Analysis

Fluoroscopic imaging of the tibiae, AP and mediolateral projections, were performed after the spacer procedure (Week 0), the graft procedure (Week 4), and followup (Week 8). Short sedation, using intramuscular injections of dexmedetomidine (0.001–0.005 mg/kg) and ketamine (2.0 mg/kg), was needed to perform the radiographs. Radiographs were obtained after euthanasia (after soft tissues were dissected) 12 weeks after the grafting procedure. The resulting images were ranked from 1 (greatest bone healing) to 29 (no healing) by two independent investigators (GFM and NSP) who were blinded to treatment allocation. Any differences in rankings between investigators were resolved after group review. The highest-ranking sites revealed bony bridging (bone extending the length of the defect with no discontinuity) of all four cortices followed by bony bridging of three, two, one, or none of the cortices. Among samples that had the same number of bony bridges, the ranking was based on the subjective amount of bone observed.

Histologic Analysis

After micro-CT data collection, histologic and histomorphometric analyses were performed. The reviewers (FT, EM, CB) were blinded to the treatment groups of the

samples being assessed. Each fixed tibia was immersed in dilute HCl (approximately 1 week) and then transferred to a 10% EDTA solution until completely decalcified. Decalcified specimens were embedded in paraffin trimmed to 7 cm to include the 5-cm defect and 1 cm at either end. The specimens were compared with the corresponding 12-week fluoroscopic radiographs taken with a BV Pulsera mobile C-ARM (Philips Medical Systems, Eindhoven, The Netherlands) to ensure that the correct tissue area was examined. The specimens then were divided into four 1.75-cm long segments that then were cut in the craniocaudal direction on the midsagittal plane to yield medial and lateral halves. Medial halves (each including the anterior and posterior cortices) were processed in paraffin (four blocks per specimen), sectioned at 5 μm , and stained with hematoxylin and eosin and Masson's trichrome. For the histomorphometric analysis, the total area of bone in the sections from the two central 1.75-cm blocks (total of 3.5 cm) was measured by tracing the perimeter of each focus per area of bone tissue in the section in the anterior and posterior cortices (mm^2) using SPOT BasicTM histomorphometry software (SPOT Imaging, Sterling Heights, MI, USA) and summing the results for each animal.

Statistical Analysis

A power analysis using previously collected data with this animal model was performed to estimate the sample size required for detecting a difference in new bone volume parameter [12, 24]. Using the traditional α set to 0.05, 16 goats (eight animals per group) provide a power of 0.78 to detect a change from 20% bone volume to 30%. This 10% difference in a 12-cm³ defect is 1.2 cm³ and was considered to be clinically significant.

We assessed bone formation 12 weeks after injury using micro-CT as the primary outcome, and radiographs and histologic analysis as secondary outcomes. Bone formation in the center 2.5 cm was defined as the primary outcome a priori in the aims, based on the expectation that the center region would be more discriminating, by eliminating the contribution of reactive bone adjacent to the osteotomy site. However, to provide data and analysis that are consistent with most conventional approaches, a secondary analysis was performed comparing total bone formation throughout the full 5-cm defect. All statistics were performed using RStudio, Version 0.98.953 (RStudio Inc, Boston, MA, USA). The final 29 goats that underwent the two surgical steps were included in the final analyses. Effects of treatments on total bone volume were assessed by using linear mixed-effect model analysis with the following equation using the *lme4* R package:

$Model = lmer(membrane\ treatment\ bone\ volume + (1|spacer), data = study\ data)$

The random effect was “*spacer*” (smooth or textured) and the fixed effect was “*membrane treatment*” (*scraped or intact*).

A two-way ANOVA for factorial design was applied to the data using the following equation:

$aov = aov(membrane\ treatment\ bone\ volume * spacer)$

This equation tests for the significances of *membrane treatment*, *spacer* and a possible relation between *membrane treatment* and *spacer* on *total bone volume* outcome. ANOVA showed no interaction between the two treatments regarding total bone volume. After pooling all goats, a t test was used to show the significance of scraping or not scraping on total bone volumes as follows: $t\text{-test}(membrane\ treatment\ bone\ volume)$.

All data are expressed as mean estimate (obtained by the mixed model), median, range between 25% percentile and 75% percentile (quartile [Q], Q1–Q3). Significance was accepted at a probability less than 0.05.

Results

Does the use of a textured spacer during the first stage of the Masquelet induced-membrane technique increase bone formation after grafting?

The use of a textured spacer did not increase new bone formation in comparison to a smooth spacer. There was no difference measured in mean radial tBV assessed by micro-CT in the 2.5 cm central region between the smooth (mean, 2473.2 mm³; median, 1143.6 mm³; Q1–Q3, 230.2–2451.1 mm³) and textured spacer (mean, 2405.5 mm³; median, 772.7 mm³; Q1–Q3, 195.9–2743.8 mm³) groups ($p = 0.917$; 95% CI, –1223.7 to 1359.0) (Fig. 2), and no difference was detected in the entire 5-cm defect region between the smooth (mean, 3501.58 mm³; median, 2351.1 mm³; Q1–Q3, 1161.0–5690.1 mm³) and textured spacer group (mean, 3367.12 mm³; median, 2304.7 mm³; Q1–Q3, 1132.2–5493.1 mm³) ($p = 0.90$) (Fig 2). Mean %BV (Fig. 3A) showed that there is qualitatively greater bone formation near the osteotomy sites. In both textured and smooth spacer groups, mean moment angle plots (Fig 3B) showed qualitatively comparable new bone formation with bone preferentially forming posteriorly in both groups. The radiographic ranking (Fig. 4) (Appendix 1. Supplemental materials are available with the online version of CORR®.) did not reveal any differences between the smooth and textured spacer groups. Histologic assessment of the goat tibia samples (Fig. 5) identified no

evidence of inflammation in any of the sections 12 weeks after grafting. The majority of new bone that was present in the sections was composed of cancellous woven bone. Defects containing little or no bone were filled primarily with fibrous connective tissue. There was no evidence of persistence of the original autogenous cancellous bone graft. Histologic analysis showed qualitatively that a comparable range of new bone area was measured in the smooth spacer group (range, 9–358 mm²) and in the textured spacer group (range, 4–980 mm²).

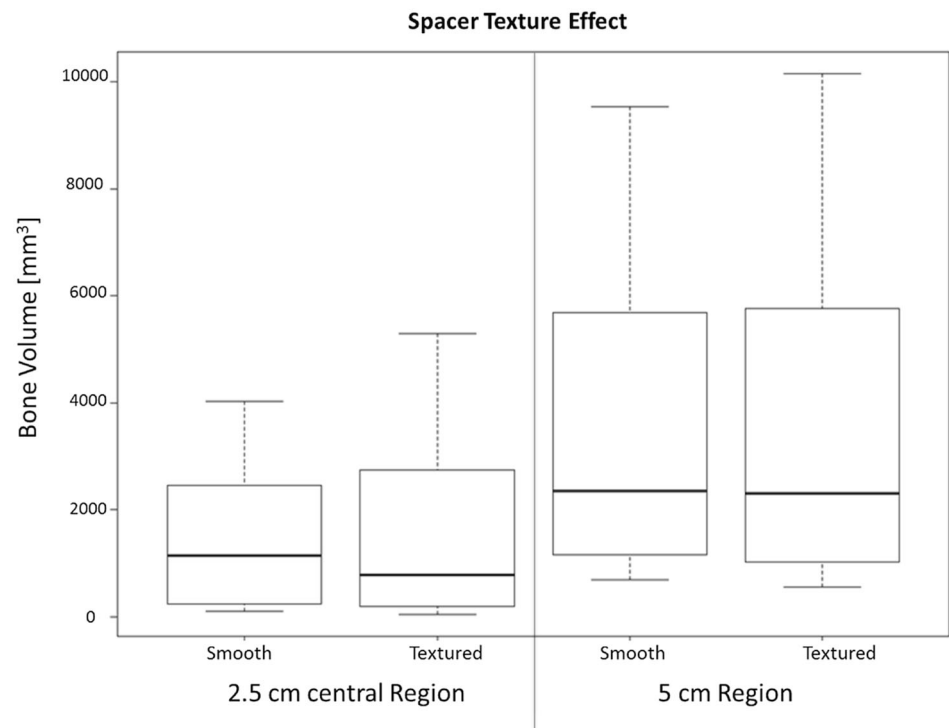
Does the surgical scraping to remove a thin (1–2 mm) layer of the inner surface of the induced membrane immediately adjacent to the spacer enhance bone formation after bone grafting?

There was greater bone formation in defects with scraped induced membrane compared with defects with intact induced membrane. Mean radial tBV in the central 2.5 cm of the defect was greater in the scraped induced-membrane group (mean, 3034.5 mm³; median, 1928.0 mm³; Q1–Q3, 273.3–2921.1 mm³) versus intact induced membrane (mean, 1709.5 mm³; median, 473.8 mm³; Q1–Q3, 132.2–1272.3 mm³; $p = 0.034$; 95% CI, –2549.0 to –101.1) (Fig. 6). When the entire 5-cm defect was considered, the mean tBV in the intact induced-membrane group was 2487.27 mm³ (median, 4570.0 mm³; Q1–Q3, 1380.9–6313.4 mm³) and mean tBV in the scraped induced-membrane group was 4208.05 mm³ (median, 1506.8 mm³; Q1–Q3, 764.6–3034.1 mm³). Post hoc one-tailed comparison of these totals using a Student’s t test (not model-based) found $p = -0.049$ (Fig. 6). The moment angle of the inertia plots (Fig. 3) shows that, qualitatively, bone tended to form along the posterior and medial aspects of the defect with little bone formation laterally in the scraped induced-membrane group, whereas in the intact induced-membrane group, new bone formation was found posteriorly. Overall, the scraped induced-membrane group ranked better than the intact induced-membrane group (Fig. 4) (Figure S1. Supplemental materials are available with the online version of CORR®.). Ten of the top 12 radiographs belonged to the scraped induced-membrane group. Histologic analysis showed qualitatively that the most-robust bone regeneration occurred in the scraped induced-membrane group (range, 4–980 mm²) compared with the intact induced-membrane group (range, 22–905 mm²), which is consistent with the micro-CT data.

Discussion

The Masquelet technique is an effective two-stage method to enhance bone reconstruction by creating a vascularized soft tissue envelope before grafting of bone defects [1, 3, 5, 8, 13, 14, 16, 23, 27]. Enhancing bone formation

Fig. 2 The box plot shows the distribution of total bone volume (based on micro-CT analyses) based on the effect of the spacer in the central 2.5 cm of the defect and the entire 5-cm defect.



with the use of the Masquelet induced-membrane method and characterization of the biologic features of the induced membrane have the potential to improve the clinical care of patients who require bone regeneration procedures to treat critical segmental bone defects. The main finding of this study was that scraping the inner surface of the induced membrane during the second stage of the Masquelet technique was associated with improved bone formation that nearly doubled the mean amount of bone formation compared with that of the control group, but a textured spacer did not appear to have the same effect.

Our study has two primary limitations. Although the process of scraping using the chronic caprine tibial defect model was associated with near doubling in bone formation when autogenous cancellous bone graft was used, the variation in the data was high and scraping did not automatically translate to clinical success. The risk of an α error (finding an effect by chance) remains close to 3%. Given the simplicity of this method and the very low risk or effort involved, we believe that it is appropriate to test this surgical technique variation in appropriately designed human clinical settings. It is also appropriate for the scraping method to be assessed in settings where other animal models using other graft materials are used to further test and confirm the value of this method in a larger range of conditions. Advancement in surgical clinical care of bone defects has been limited because available large animal models generally have acute bone defects in young healthy animals that heal reliably with

many existing therapies, creating a “ceiling effect” [19]. The chronic caprine tibial defect model addresses the latter limitation and provides a robust model that “raises the bar” for rigorous assessment of bone grafting strategies by including the biologic features of muscle injury, loss of periosteum, bone marrow reaming, and local scar formation, which are missing in traditional acute large animal models. Even autogenous cancellous bone grafts in the animals in this study achieved a mean of only 4 cm³ of new bone in a 12-cm³ defect site. Therefore, these features better model the challenging biologic environment where advancement needs to be made and documented. In addition, the use of 4- to 6-year-old goats provides a model of middle-aged animals that is more reflective of the clinical environment, in contrast to many models which use young adolescent animals which generally have superior bone regeneration potential. The most-sensitive test for new bone formation is in the center-most 2.5 cm of the bone defect, eliminating reactive bone formation that may occur independent from the grafting strategy. Furthermore, histologic analysis was used as a secondary outcome to evaluate and confirm the quality of the new bone tissue formed. Biomechanical testing was not used as an outcome parameter in this dataset, because the frequency of bone union was low. In the absence of bone regeneration, the mechanical performance of these defects was obviously insufficient. Biomechanical testing will be of future value, as better grafting methods are used, and the frequency of union becomes greater.

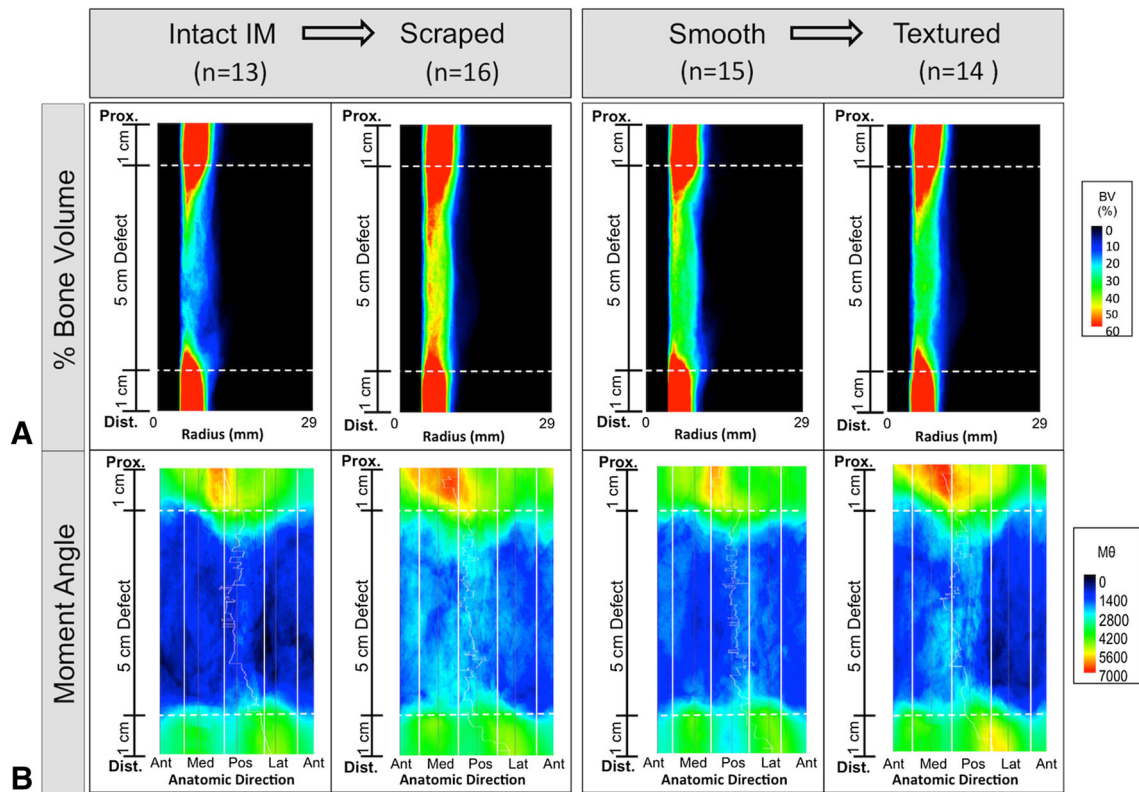
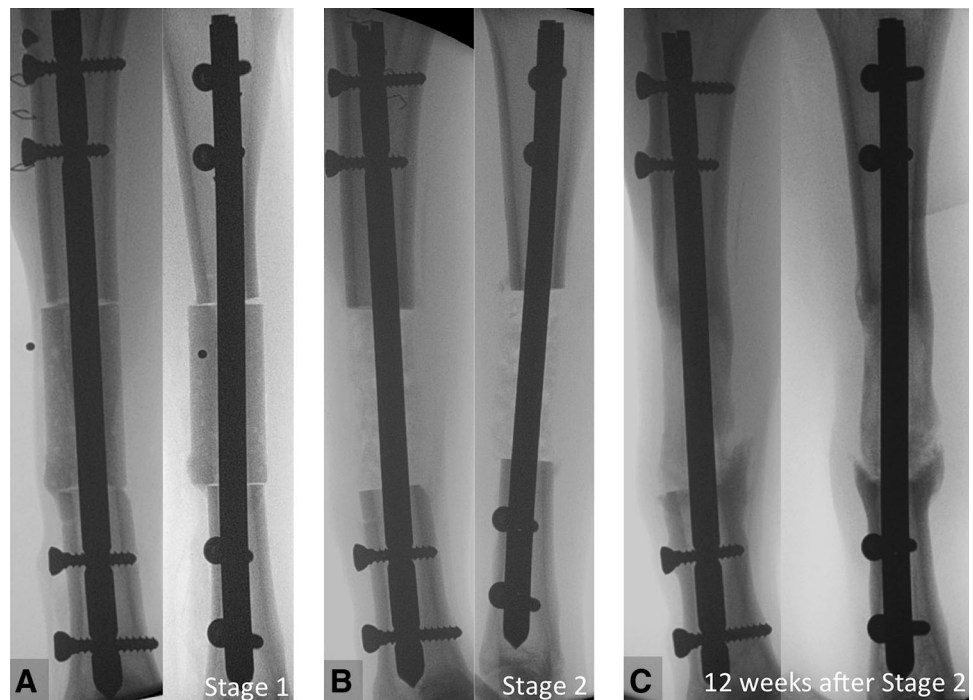


Fig. 3A–B Mean micro-CT plots show the differences in bone formation and distribution. (A) A radial color plot shows the bone formation (% bone volume [BV]) as the summation of the radial location relative to vertical position in the defect. More %BV (red/yellow) is appreciated in the scraped group compared with the intact

induced-membrane (IM) group. (B) A moment angle ($M\theta$ ($HU \cdot mm^2$)) plot shows that most bone formed on the posterior aspect of this defect. The proximal and distal borders of the defect are marked by dashed lines. Prox. = proximal; Dist. = distal; Ant = anterior; Med = medial; Pos = posterior; Lat = lateral.

Fig. 4A–C Representative AP and lateral views of fluoroscopic images taken (A) after the “spacer procedure” (Stage 1) show the polymethylmethacrylate spacer in the defect site; (B) after the “graft procedure” (Stage 2) 4 weeks later show autogenous cancellous bone graft in the defect; and (C) at the time of euthanasia (12 weeks after Stage 2) show new bone formation in the defect.



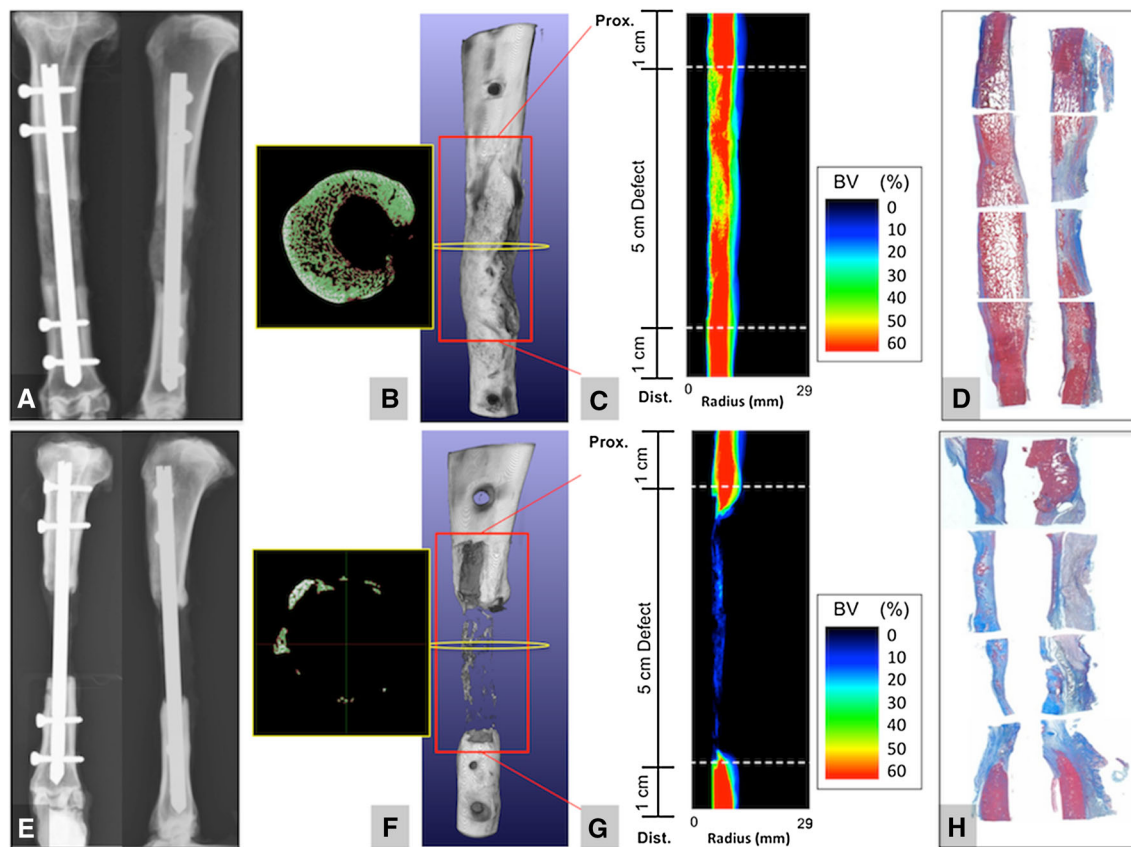


Fig. 5A–H Examples of two representative study goats are presented. One goat showed robust bone formation on (A) postmortem AP and lateral view, (B) micro-CT 3-D reconstruction and axial image (yellow box), (C) % bone volume (BV) plot versus summation of radial position, and on (D) Masson's trichrome-stained histology slides (pink staining shows substantial bone formation). And another

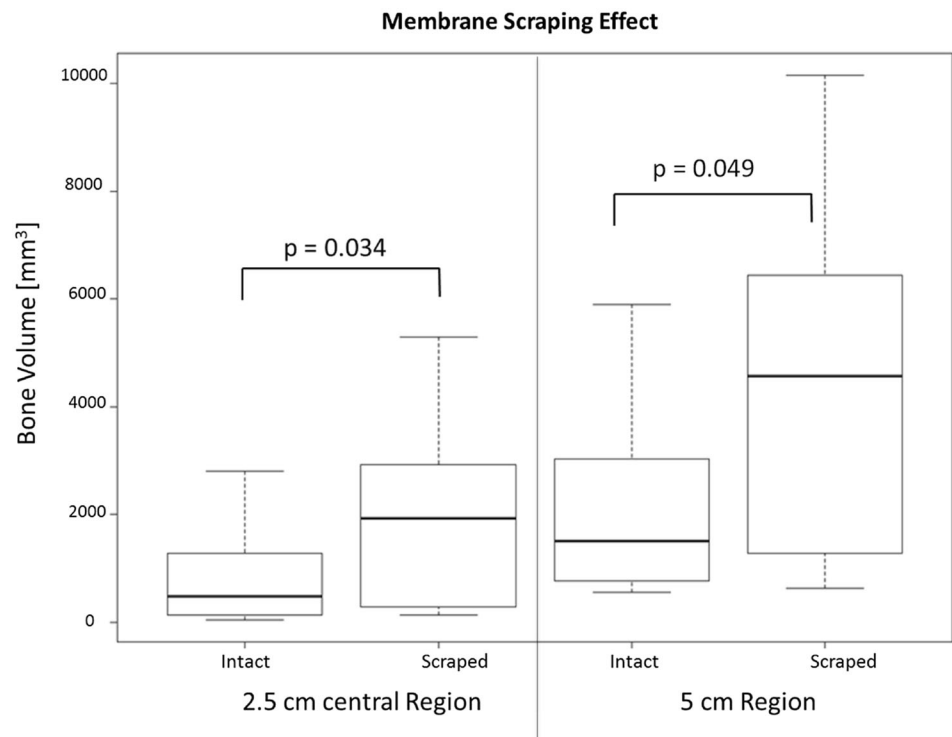
goat showed minimal new bone formation on (E) postmortem AP and lateral radiographs, (F) micro-CT 3-D reconstruction and axial image (yellow box), (G), % bone volume (BV) plot versus summation of radial position, and on (H) Masson's trichrome-stained histology slides (pink staining shows substantial bone formation).

A textured spacer has been reported to be associated with more-developed membrane synoviallike metaplasia and villous hyperplasia [14], but the effect of spacer texture on bone healing is not well known. In the current study, we tested a ribbed spacer that doubled the induced-membrane surface area to try to enhance bone healing; however, we did not find a difference in bone volume between the two spacer designs. However, there are many other texture options that may be considered before texture should be discarded as a possible opportunity for improvement. Other variables that will require further research with the potential to increase bone formation or shorten the time to obtain bone union with the Masquelet technique that may be considered are: spacer bulk materials (eg, other polymers in addition to PMMA), variation in time allotted to each stage, delivery of growth factors using a spacer, type and amount of grafting material, and supplementation with cell-based therapies [3, 14, 18, 26, 28].

Although the Masquelet technique is used worldwide [7] and a substantial amount of basic and clinical research has

been done on the induced-membrane technique, there are no established surgical standards to manage the induced-membrane inner surface before bone grafting. Our study showed that scraping the inner surface of the induced membrane enhanced new bone formation. The induced membrane is composed of two portions: a thin glistening inner surface, comprised of protein exudate and mild foreign body reaction, and an outer part made of fibroblasts, myofibroblasts, and collagen [22]. This inner surface has been described as an organized, richly vascularized, pseudosynovial membrane that promotes revascularization of the graft that is contained in the membrane and prevents its resorption [10, 14, 22, 28]. Removal of this glistening inner layer of the induced membrane induces bleeding from a healthy vascular bed while preserving the mechanical function of the rest of the fibrous envelope of the induced membrane. This technical surgical modification may represent a rapid and simple means of enhancing the biologic environment of the tissue bed. Further investigation into the nature of the induced

Fig. 6A–B The box plots show the distribution of total bone volume (based on micro-CT analyses) based on intact membrane or membrane scraped in the (A) central 2.5 cm of the defect (left) and the (B) entire 5-cm defect (right). The scraped induced-membrane group showed higher total bone volume compared with the intact membrane group in the 2.5 cm region ($p = 0.034$), confirming the hypothesis based on the primary outcome parameter. Post hoc (nonmodel based) comparison of tBV in the entire 5 cm defect using a one tailed t test found $p = 0.049$.



membrane including exploring differences in resident cell populations and difference in gene expression between superficial and deep zones in the induced membrane may help define a mechanism for this effect.

In this *in vivo* animal model, we found that, when using the Masquelet technique, scraping to remove the inner surface of the induced membrane before bone grafting may improve clinical bone regeneration. Scraping the inner surface of the induced membrane increases bleeding from a healthy vascular fibrous tissue bed and removes a layer of tissue associated with a foreign body reaction while preserving the mechanical function of the induced membrane as a fibrous envelope. This study highlights the opportunity to increase the amount of bone formed by modifying surgical techniques to improve healing of segmental bone defects. A new rigorous chronic caprine tibial defect model is described, that is suited for advanced preclinical assessment of bone regeneration materials and strategies for treatment of segmental bone defects. The findings from this study can be translated to clinical studies of the care of civilian and military patients. Future clinical trials need to test the clinical effect of scraping the inner surface of the induced membrane.

Acknowledgments We thank Cynthia Boehm BS, Wesley Bova BS, Maha Qadam PhD, Venkata Mantripragada PhD, and Terry Zachos MD (all from Biomedical Engineering, Cleveland Clinic) for technical assistance during surgery; Kimerly Powell PhD (Department of Biomedical Informatics, Ohio State University) and Justin Jeffery PhD (Small Animal Imaging Facility, University of Wisconsin) for help with micro-CT processing and analysis; Ferenc Toth

DVM, Elizabeth Marchant DVM, and Channing Bancroft DVM (all from the Department of Veterinary Population Medicine, University of Minnesota) for help with histology processing and analysis; and John Tra PhD (Orthopaedics Department, Walter Reed National Military Medical Center) for assistance with statistical analysis.

References

1. Aparid T, Bigorre N, Cronier P, Duteille F, Bizot P, Massin P. Two-stage reconstruction of post-traumatic segmental tibia bone loss with nailing. *Orthop Traumatol Surg Res.* 2010;96:549–553.
2. Ashman O, Phillips AM. Treatment of non-unions with bone defects: which option and why? *Injury.* 2013;44(suppl 1):S43–S45.
3. Aurégan JC, Bégué T. Induced membrane for treatment of critical sized bone defect: a review of experimental and clinical experiences. *Int Orthop.* 2014;38:1971–1978.
4. Brown KV, Guthrie HC, Ramasamy A, Kendrew JM, Clasper J. Modern military surgery: lessons from Iraq and Afghanistan. *J Bone Joint Surg Br.* 2012;94:536–543.
5. Chong KW, Woon CY, Wong MK. Induced membranes: a staged technique of bone-grafting for segmental bone loss: surgical technique. *J Bone Joint Surg Am.* 2011;93(suppl 1):85–91.
6. Domic-Cule I, Pecina M, Jelic M, Jankolija M, Popek I, Grgurevic L, Vukicevic S. Biological aspects of segmental bone defects management. *Int Orthop.* 2015;39:1005–1011.
7. Giannoudis PV. Has the induced membrane technique revolutionized the treatment of bone defects? *Tech Orthop.* 2016;31:2.
8. Giannoudis PV, Faour O, Goff T, Kanakaris N, Dimitriou R. Masquelet technique for the treatment of bone defects: tips-tricks and future directions. *Injury.* 2011;42:591–598.
9. Grass M, Köhler T, Proksa R. 3D cone-beam CT reconstruction for circular trajectories. *Phys Med Biol.* 2000;45:329–347.
10. Klaue K, Knothe U, Anton C, Pfluger H, Stoddart M, Masquelet AC, Perren SM. Bone regeneration in long-bone defects: tissue

- compartmentalisation? In vivo study on bone defects in sheep. *Injury*. 2009;40(suppl 4):S95–102.
11. Lasanianos NG, Kanakaris NK, Giannoudis P V. Current management of long bone large segmental defects. *Orthop Trauma*. 2010;24:149–163.
 12. Luangphakdy V, Boehm C, Pan H, Nicholson C, Carloson J, Bechtold J, Pluhar E, Muschler G. Characterization of the Chronic Caprine Tibial Defect Model. Tissue Engineering International & Regenerative Medicine Society. *TERMIS Annual Meeting*. Washington, DC, USA, December 14–16, 2014.
 13. Masquelet AC. The evolution of the induced membrane technique: current status and future directions. *Tech Orthop*. 2016; 31:3–8.
 14. Masquelet AC, Begue T. The concept of induced membrane for reconstruction of long bone defects. *Orthop Clin North Am*. 2010;41:27–37.
 15. Masquelet AC, Fitoussi F, Begue T, Muller GP. [Reconstruction of the long bones by the induced membrane and spongy autograft][in French]. *Ann Chir Plast Esthet*. 2000;45:346–353.
 16. Masquelet AC, Obert L. [Induced membrane technique for bone defects in the hand and wrist][in French]. *Chir Main*. 2010;29(-suppl 1):S221–224.
 17. Mauffrey C, Barlow BT, Smith W. Management of segmental bone defects. *J Am Acad Orthop Surg*. 2015;23:143–153.
 18. Mauffrey C, Hake ME, Chadayammuri V, Masquelet AC. Reconstruction of long bone infections using the induced membrane technique: tips and tricks. *J Orthop Trauma*. 2016;30: e188–193.
 19. Muschler GF, Raut VP, Patterson TE, Wenke JC, Hollinger JO. The design and use of animal models for translational research in bone tissue engineering and regenerative medicine. *Tissue Eng Part B Rev*. 2010;16:123–145.
 20. National Research Council. *Guide for the Care and Use of Laboratory Animals*. 8th ed. Washington, DC: National Academies Press; 2011.
 21. Owens BD, Kragh JF Jr, Macaitis J, Svoboda SJ, Wenke JC. Characterization of extremity wounds in Operation Iraqi Freedom and Operation Enduring Freedom. *J Orthop Trauma*. 2007;21:254–257.
 22. Pelissier P, Masquelet AC, Bareille R, Pelissier SM, Amedee J. Induced membranes secrete growth factors including vascular and osteoinductive factors and could stimulate bone regeneration. *J Orthop Res*. 2004;22:73–79.
 23. Pipitone PS, Rehman S. Management of traumatic bone loss in the lower extremity. *Orthop Clin North Am*. 2014;45:469–482.
 24. Pluhar E, Luangphakdy V, Boehm C, Shinohara K, Pan H, Carlson C, Muschler G. Effect of Grafting Materials on Bone Healing in a Chronic Caprine Tibial Defect Model. *Military Health System Research Symposium*. August 18–21, 2014, Fort Lauderdale, FL, USA.
 25. Pneumaticos SG, Triantafyllopoulos GK, Basdra EK, Papavasiliou AG. Segmental bone defects: from cellular and molecular pathways to the development of novel biological treatments. *J Cell Mol Med*. 2010;14:2561–2569.
 26. Pountos I, Panteli M, Jones EA, Giannoudis PV. How the induced membrane contributes to bone repair. *Tech Orthop*. 2016;31:9–13.
 27. Ronga M, Ferraro S, Fagetti A, Cherubino M, Valdatta L, Cherubino P. Masquelet technique for the treatment of a severe acute tibial bone loss. *Injury*. 2014;45(suppl 6):S111–115.
 28. Viateau V, Bensedhoum M, Guillemin G, Petite H, Hannouche D, Anagnostou F, Pelissier P. Use of the induced membrane technique for bone tissue engineering purposes: animal studies. *Orthop Clin North Am*. 2010;41:49–56.